

Supporting Information

Unprecedented (μ -1,1-Peroxo)diferric Structure for the Ambiphilic Orange Peroxo Intermediate of the Nonheme N-Oxygenase CmII

Andrew J. Jasniewski,^{†,‡,§,#} Anna J. Komor,^{†,‡,§,#} John D. Lipscomb,^{*,§,‡} and Lawrence Que, Jr.^{*,†,‡}

[†]Department of Chemistry, [§]Department of Biochemistry Molecular Biology, and Biophysics, and [‡]Center for Metals in Biocatalysis, University of Minnesota, Minneapolis, Minnesota 55455

Joint First Authors

[#]Contributed equally to the study

***Corresponding authors**

J.D.L.: Tel: (612) 625-6454; Fax, (612) 624-5121; E-mail, lipsc001@umn.edu

L. Q.: Tel: (612) 625-0389; Fax, (612) 625-7029; E-mail, larryque@umn.edu

Table of Contents	Page Number
Figure S1. Pre-edge region analysis of Cmll ^R	3
Figure S2. Pre-edge region analysis of Cmll ^{Ox}	4
Figure S3. Pre-edge region analysis of Cmll ^P	5
Figure S4. EXAFS data of Cmll ^R	6
Table S1. Fit parameters for Cmll ^R	7
Figure S5. EXAFS data of Cmll ^{Ox}	8
Table S2. Fit parameters for Cmll ^{Ox}	9
Figure S6. EXAFS data of Cmll ^P	10
Table S3. Fit parameters for Cmll ^P	11
Table S4. Component Analysis of Pre-edge of Cmll	13
Figure S7. Full resonance Raman spectra for Cmll ^{Ox} and Cmll ^P	14

General EXAFS considerations. In the fit tables of EXAFS data, N refers to the number of scatterers used for a particular shell, R is the distance of the scattering shell, σ^2 is the mean-squared deviation (or Debye-Waller factor), E_0 is the edge shift parameter, and the goodness of fit (GOF) parameters are calculated as $F = \sqrt{\sum k^6 (\chi_{\text{exp}} - \chi_{\text{calc}})^2}$, $F' = \sqrt{\sum k^6 (\chi_{\text{exp}} - \chi_{\text{calc}})^2 / \sum k^6 \chi_{\text{exp}}^2}$. For all fits, the amplitude reduction factor (S_0^2) was set to 0.9.

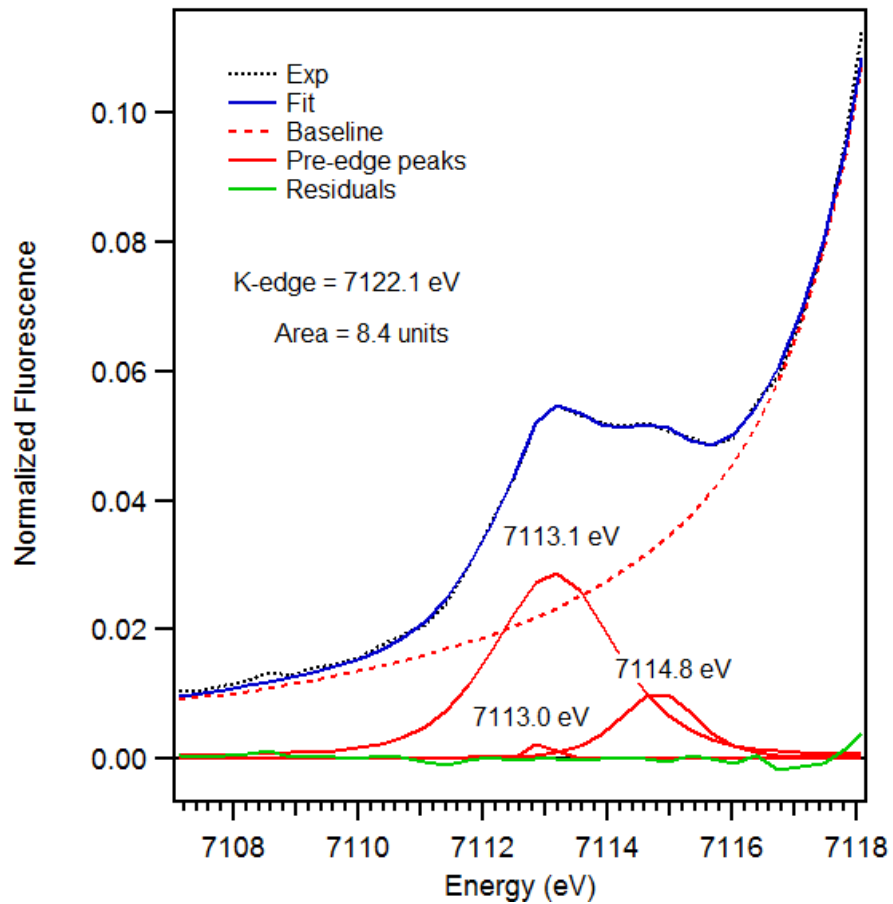


Figure S1. Pre-edge region analysis of Cmll^R. The experimental data (black dotted), baseline (red dashed), pre-edge peak components (red solid), residuals (green solid), and total fit (blue solid) are shown.

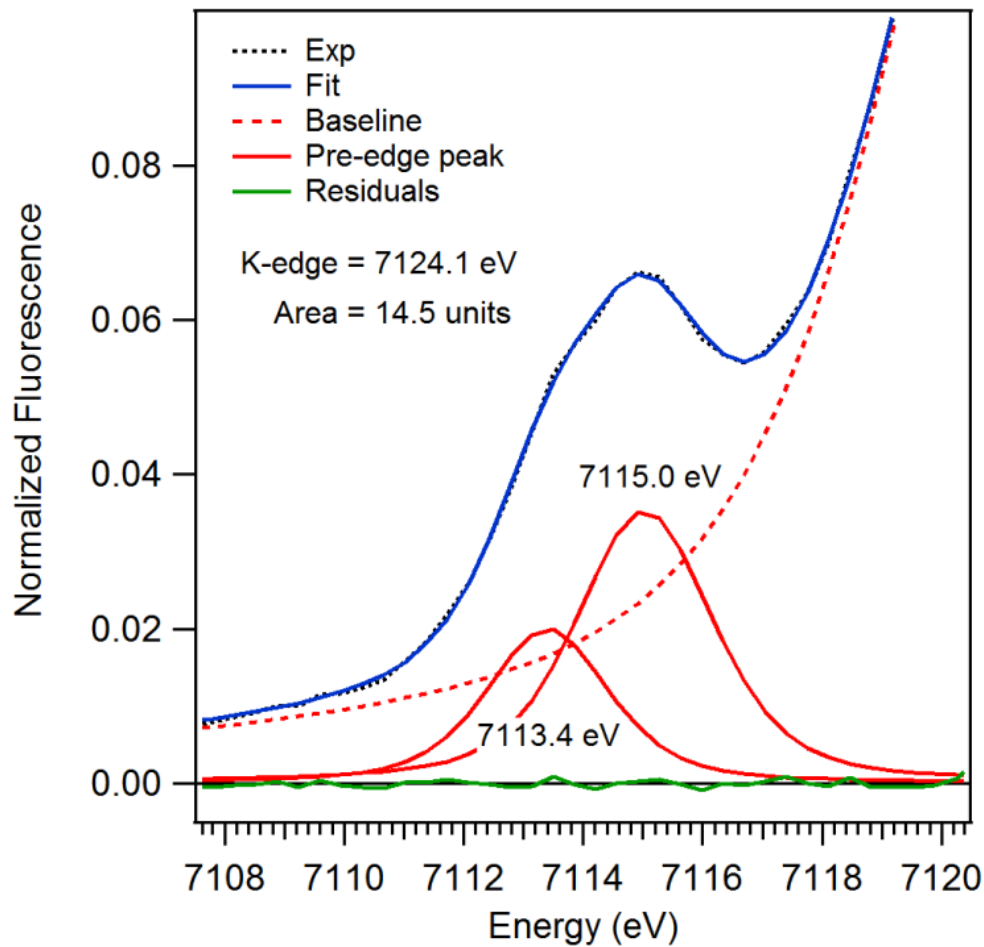


Figure S2. Pre-edge region analysis of CmII^{Ox} . The experimental data (black dotted), baseline (red dashed), pre-edge peak components (red solid), residuals (green solid), and total fit (blue solid) are shown.

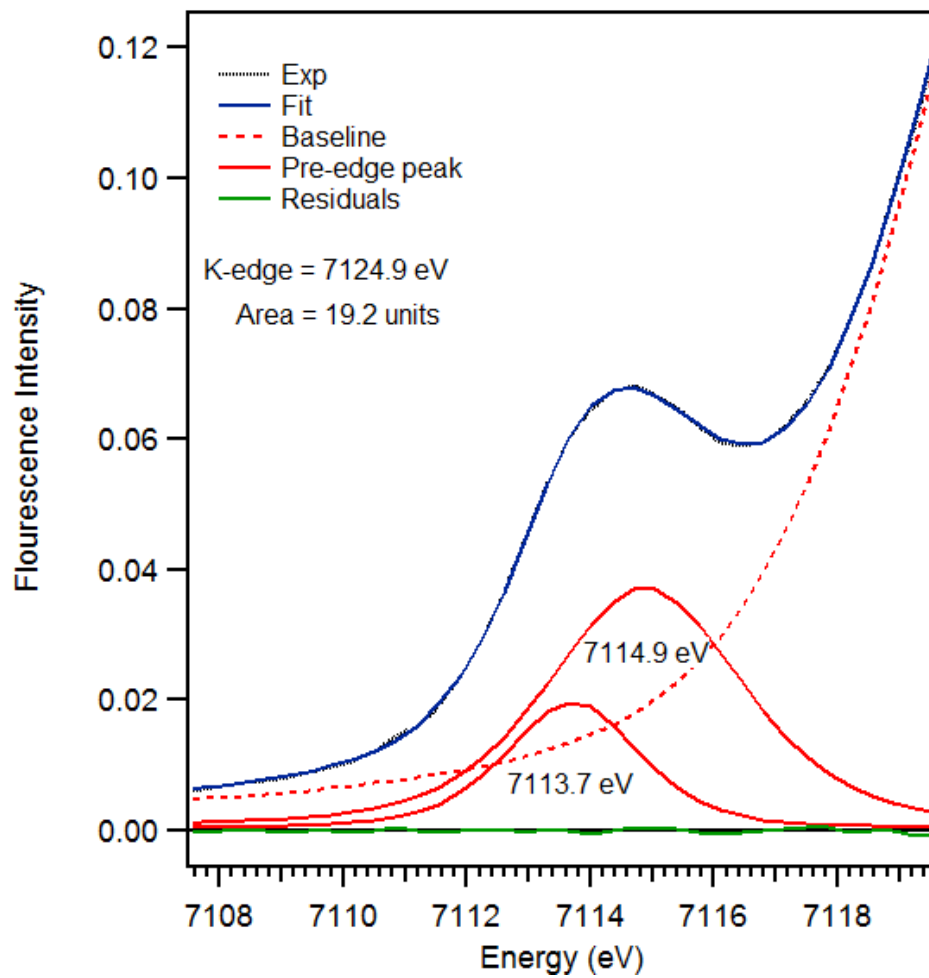


Figure S3. Pre-edge region analysis of CmII^{P} . The experimental data (black dotted), baseline (red dashed), pre-edge peak components (red solid), residuals (green solid) and total fit (blue solid) are shown.

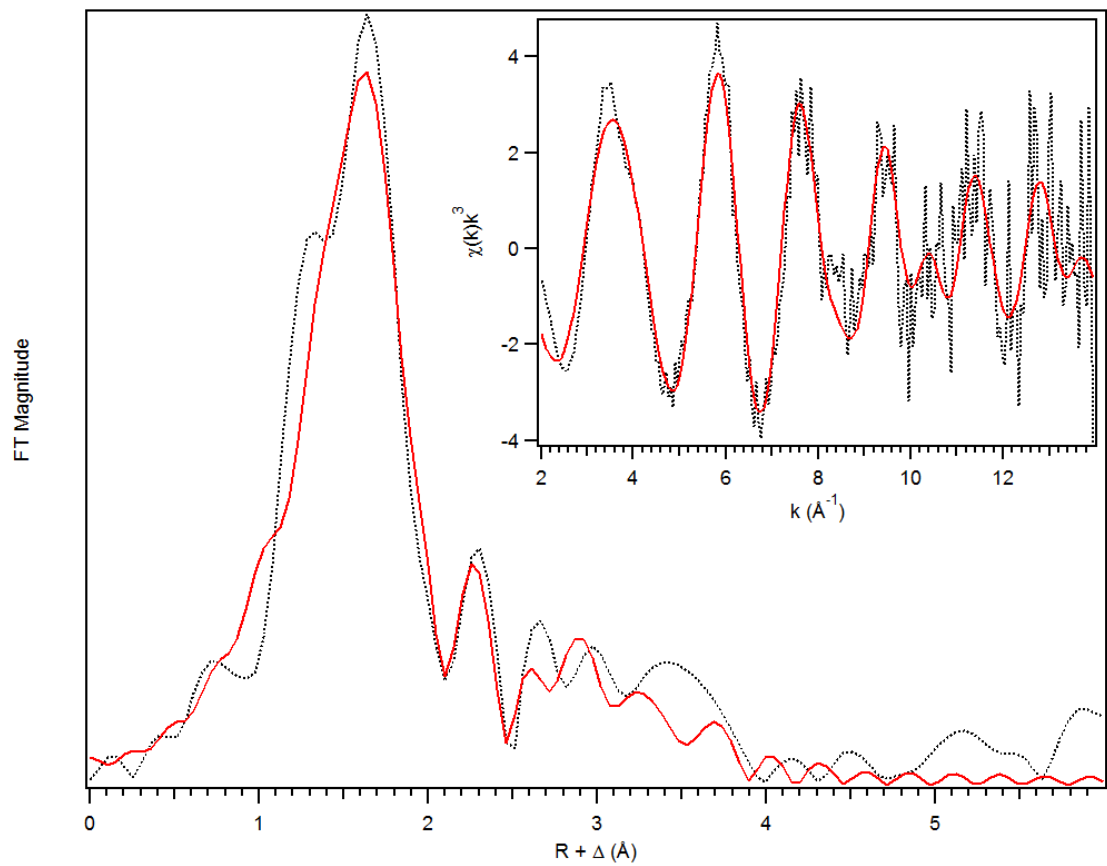


Figure S4. Fit (red solid line) of the unfiltered (black dotted) EXAFS data (inset) and corresponding Fourier transform of $\mathbf{Cmll}^\mathbf{R}$ (Table S1, Fit 17). Data was fit between $k = 2\text{--}14 \text{\AA}^{-1}$.

Table S1. Fit parameters for the unfiltered EXAFS data of CmII^R, between $k = 2 - 14 \text{ \AA}^{-1}$.

Fit 17 gives the most reasonable fit of the experimental data.

	Fe-N				Fe-O				Fe $\cdots\cdots$ Fe				Fe $\cdots\cdots$ C				GOF	
Fit	N	R(Å)	$\sigma^2(10^{-3})$	N	R(Å)	$\sigma^2(10^{-3})$	N	R(Å)	$\sigma^2(10^{-3})$	N	R(Å)	$\sigma^2(10^{-3})$	E _o	F	F'			
1	6	2.10	7.61										-10.3	300	568			
2	5	2.10	6.23										-9.53	304	572			
3	4	2.11	4.81										-8.82	323	590			
4	3	2.11	3.31										-8.22	365	627			
5	3	2.12	2.60	1	2.01	2.03							-9.71	304	572			
6	4	2.11	4.06	1	1.98	4.40							-11.2	288	557			
7	5	2.10	4.99	1	1.94	5.01							-12.8	281	550			
8	4	2.11	4.03	2	1.97	7.33							-13.6	274	544			
9	4	2.13	4.87	1	2.02	4.61				3	3.11	4.20	-8.72	257	527			
10	4	2.12	4.83	1	2.01	6.35				3	3.14	0.93	-9.05	240	509			
										3	2.99	3.97						
11	4	2.12	4.76	1	2.00	5.61				3	3.15	0.87	-9.66	226	493			
										3	2.99	3.68						
										1	2.59	1.38						
12	4	2.12	4.76	1	2.01	4.90	1	3.34	9.20	3	2.99	2.77	-8.88	221	487			
										5	3.15	2.08						
										1	2.60	0.85						
13	4	2.12	5.01	1	2.01	5.90	1	3.35	9.54	5	3.15	2.62	-9.10	210	475			
										3	2.99	3.50						
										1	2.60	1.41						
										4	4.01	1.06						
14	4	2.12	4.80	1	2.00	5.54				5	3.13	3.88	-9.61	217	484			
										3	2.96	4.31						
										1	2.60	2.07						
										4	4.02	1.30						
15	4	2.12	4.91	1	2.01	6.72	1	3.34	9.73	5	3.15	2.23	-9.04	223	490			
										3	2.99	3.16						
										4	4.00	1.49						
16	4	2.13	5.11	1	2.02	3.96	1	3.38	10.36	5	3.13	7.48	-8.09	227	495			
										4	4.02	1.32						
										1	2.61	1.36						
17	5	2.10	5.02	1	1.94	5.35	1	3.35	9.90	1	2.58	1.35	-12.0	206	470			
										3	2.98	2.76						
										5	3.14	2.48						
										4	3.99	1.15						
18	4	2.11	4.71				1	3.35	8.37	1	2.60	1.08	-7.27	233	501			
										3	3.00	2.37						
										5	3.16	1.74						
										4	4.02	0.75						

Table S1 (continued). Fit parameters for the unfiltered EXAFS data of **Cmll^R**, between $k = 2 - 14 \text{ \AA}^{-1}$. Fit 17 gives the most reasonable fit of the experimental data.

Fe-N				Fe-O				Fe...Fe				Fe...C				GOF	
Fit	N	R(Å)	$\sigma^2(10^{-3})$	N	R(Å)	$\sigma^2(10^{-3})$	N	R(Å)	$\sigma^2(10^{-3})$	N	R(Å)	$\sigma^2(10^{-3})$	E _o	F	F'		
19	5	2.11	4.75	1	1.94	4.36	1	3.34	8.55	0.5	2.58	-2.50	-11.7	198	462		
										3	2.99	1.03					
										5	3.14	1.15					
										4	3.99	3.31					

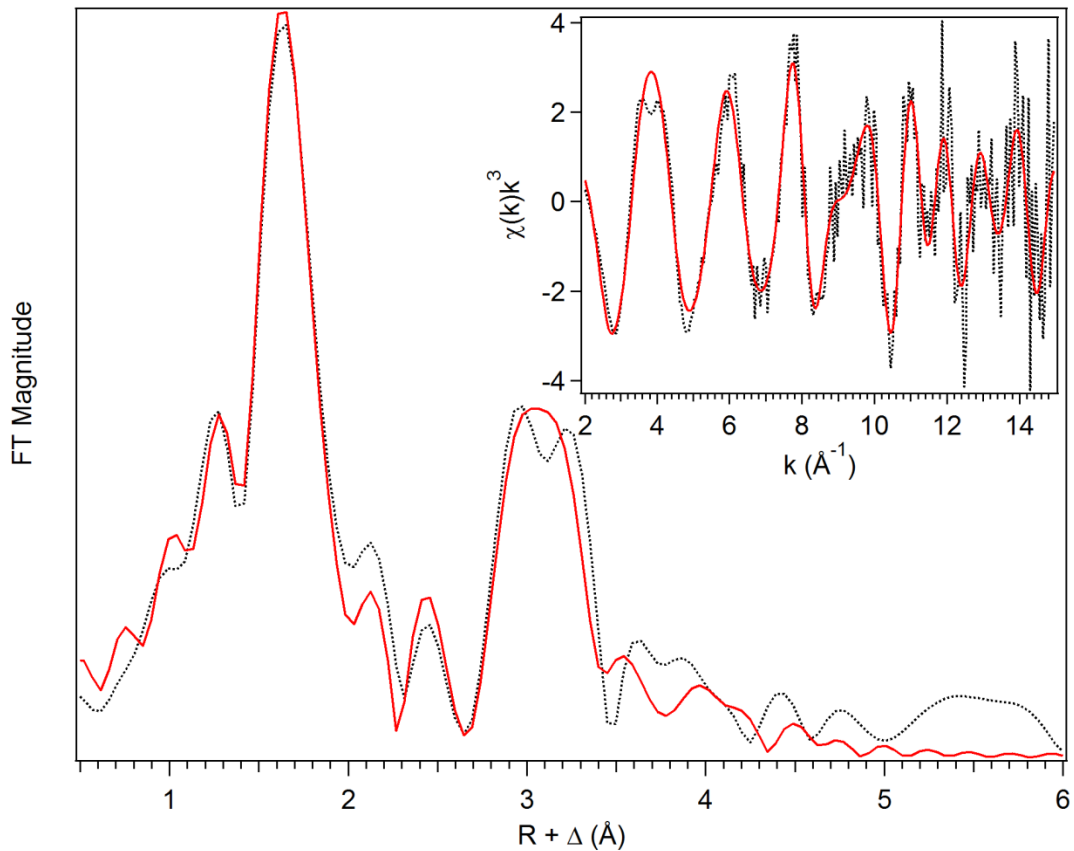


Figure S5. Fit (red solid line) of the unfiltered (black dotted) EXAFS data (inset) and corresponding Fourier transform of **Cmll^{Ox}** (Table S2, Fit 15). Data was fit between $k = 2 - 15 \text{ \AA}^{-1}$.

Table S2. Fit parameters for the unfiltered EXAFS data of **CmII^{Ox}**, between $k = 2 - 15 \text{ \AA}^{-1}$. Fit 15 gives the most reasonable fit of the experimental data. The Fe \cdots C shells at 3.57 and 4.28 \AA are consistent with bound His ligands.

Fit	Fe-N				Fe-O				Fe \cdots Fe				Fe \cdots C				GOF		
	N	R(\AA)	$\sigma^2(10^{-3})$	N	R(\AA)	$\sigma^2(10^{-3})$	N	R(\AA)	$\sigma^2(10^{-3})$	N	R(\AA)	$\sigma^2(10^{-3})$	E _o	F	F'				
1	6	2.11	10.64										0.50	408	704				
2	5	2.11	8.68										1.22	388	687				
3	4	2.12	6.92										1.88	383	682				
4	3	2.12	5.26										2.46	404	701				
5	4	2.11	6.58	1	1.95	18.06							-0.27	378	678				
6	3	2.17	2.44	1	2.03	-0.50							2.26	3.57	659				
7	3	2.18	4.56	2	2.04	3.92							1.33	388	687				
8	3	2.16	1.74	2	2.02	0.74							-2.42	331	635				
				1	1.84	3.15													
9	3	2.16	1.96	2	2.02	0.94	1	3.31	2.52				-1.78	248	550				
				1	1.85	3.63													
10	3	2.17	2.19	2	2.03	1.16	1	3.31	2.35	2	3.12	3.67	-0.76	239	538				
				1	1.85	4.45													
11	3	2.15	1.82	2	2.01	0.98	1	3.31	3.20	2	3.07	10.44	-2.85	209	504				
				1	1.84	3.08							3	3.57	1.14				
12	3	2.16	1.77	2	2.01	0.99	1	3.32	3.53	2	3.06	9.28	-2.39	190	481				
				1	1.84	3.22							3	3.58	0.55				
													3	4.29	1.07				
13	3	2.15	1.79	2	2.01	0.99	1	3.32	3.22	2	3.07	10.95	-2.65	191	481				
				1	1.84	3.16							4	3.57	1.70				
													3	4.29	1.18				
14	3	2.17	2.10	2	2.03	1.11	1	3.31	2.40	2	3.12	3.36	-0.74	230	528				
				1	1.85	4.28							3	4.31	3.17				
15	3	2.15	1.73	2	2.00	0.97	1	3.32	3.38	4	3.57	1.39	-3.79	196	488				
				1	1.83	2.71							3	4.28	1.04				

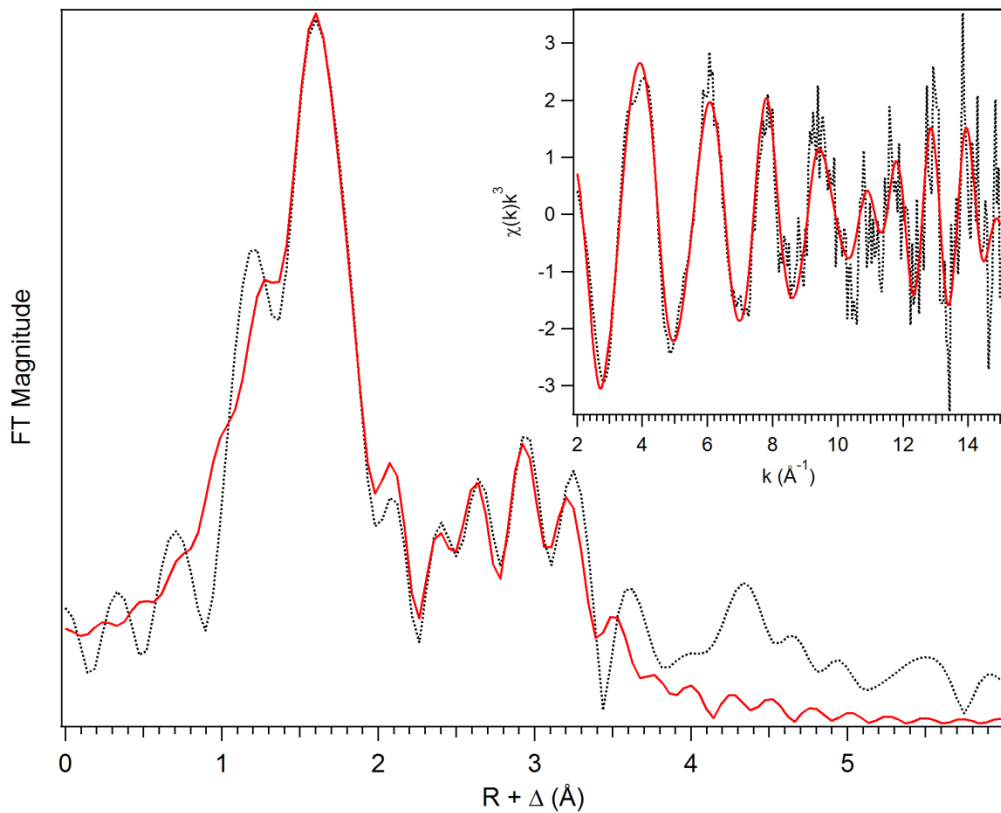


Figure S6. Fit (red solid line) of the unfiltered (black dotted) EXAFS data (inset) and corresponding Fourier transform of **CmllP** (Table S3, Fit 23). Data was fit between $k = 2 - 15 \text{\AA}^{-1}$.

Table S3. Fit parameters for the unfiltered EXAFS data of CmII^P, between $k = 2 - 15 \text{ \AA}^{-1}$.

Fit 23 gives the most reasonable fit of the experimental data.

Fit	Fe-N			Fe-O			Fe...Fe			Fe...C			GOF		
	N	R(Å)	$\sigma^2(10^{-3})$	N	R(Å)	$\sigma^2(10^{-3})$	N	R(Å)	$\sigma^2(10^{-3})$	N	R(Å)	$\sigma^2(10^{-3})$	E_o	F	F'
1	5	2.08	12.13										1.63	202	615
2	4	2.09	9.45										2.62	199	610
3	3	2.10	6.99										3.64	211	629
4	5	2.08	9.28	1	1.86	9.72							-0.65	188	594
5	5	2.08	8.96	2	1.86	14.71							-2.53	190	599
6	4	2.10	7.67	1	1.91	9.84							0.24	187	593
7	4	2.10	7.77	2	1.91	15.33							-1.50	187	592
8	3	2.12	5.25	1	1.97	4.90							1.71	191	599
9	3	2011	6.41	2	1.96	13.93							-0.59	187	593
10	3	2.13	2.58	2	1.98	2.05							-3.21	175	573
				1	1.82	3.58									
11	3	2.12	2.10	1	1.99	-0.20							-3.64	176	574
				2	1.88	9.04									
12	3	2.12	2.54	2	1.97	1.97	1	2.83	17.88				-3.29	172	568
				1	1.82	3.39									
13	3	2.13	2.54	2	1.98	1.98	1	3.37	35.99				-3.14	175	572
				1	1.82	3.54									
14	3	2.13	3.32	2	1.99	2.76	1	3.11	21.89				-2.23	154	536
				1	1.83	4.53									
				1	2.83	0.21									
15	3	2.13	2.72	2	1.98	2.53	1	3.29	10.99	1	3.11	-2.30	-2.29	124	483
				1	1.82	4.54									
				1	2.82	3.75									
16	3	2.14	3.22	2	1.99	3.02	1	3.30	6.34	3	3.12	1.69	-0.99	133	499
				1	1.83	5.44									
				1	2.84	1.50									
17	3	2.13	2.84	2	1.98	2.50	1	3.11	7.61	3	3.34	0.91	-2.36	122	478
				1	1.83	4.47									
				1	2.83	1.23									
18	3	2.13	2.41	2	1.98	1.98	1	3.34	4.23	3	3.14	4.38	-2.40	118	469
				1	1.82	3.80				3	3.55	1.85			
				1	2.82	1.81									
19	3	2.12	6.25	2	1.96	12.77	1	3.30	5.03	3	3.12	1.55	0.43	130	494
				1	2.85	1.14				3	3.49	9.49			
20	3	2.13	1.98	2	1.97	1.52	1	3.33	2.88	3	3.15	2.58			
				1	1.8	3.09									
21	3	2.13	2.81	2	1.98	2.45	1	3.1	7.66	3	3.34	0.90	-2.42	118	470
				1	1.82	4.36				3	3.78	23.62			
				1	2.83	1.22									

Table S3 (continued). Fit parameters for the unfiltered EXAFS data of **CmII^P**, between $k = 2 - 15 \text{ \AA}^{-1}$. Fit 23 gives the most reasonable fit of the experimental data. The Fe \cdots C shells at 3.14, 3.56 and 4.28 Å are consistent with bound His ligands.

Fit	Fe-N				Fe-O				Fe \cdots Fe				Fe \cdots C				GOF		
	N	R(Å)	$\sigma^2(10^{-3})$	N	R(Å)	$\sigma^2(10^{-3})$	N	R(Å)	$\sigma^2(10^{-3})$	N	R(Å)	$\sigma^2(10^{-3})$	E _o	F	F'				
22	3	2.13	2.47	2	1.98	2.03	1	3.34	4.44	3	3.14	4.84	-2.11	109	451				
				1	1.83	3.93				3	3.56	1.65							
				1	2.82	1.54				3	4.39	4.64							
23	3	2.13	2.50	2	1.98	2.09	1	3.35	4.47	3	3.14	4.87	-1.86	111	456				
				1	1.83	4.05				3	3.56	1.46							
				1	2.82	1.50				3	4.28	5.12							
24	3	2.13	2.43	2	1.97	1.95	1	3.12	8.77	3	3.34	0.43	-3.59	116	465				
				1	1.82	3.50				3	3.54	8.78							
				1	2.82	1.47				3	4.08	14.75							
25	3	2.14	2.89	2	1.99	2.52	1	3.57	7.75	3	3.12	4.61	-177	113	459				
				1	1.83	4.66				3	3.34	1.43							
				1	2.82	0.98				3	3.97	5.76							
26	3	2.13	2.05	2	1.98	1.66	1	3.33	3.03	3	3.15	2.90	-2.79	130	493				
				1	1.82	3.51				3	3.54	1.85							
										3	4.25	4.99							
27	3	2.14	3.25	2	1.99	3.03	1	3.30	6.45	3	3.12	1.71	-0.87	131	496				
				1	1.84	5.59				3	4.29	8.00							
				1	2.84	1.43													
28	3	2.14	3.38	2	1.99	2.97				3	3.09	3.59	-1.24	142	516				
				1	1.84	5.24				3	3.60	2.10							
				1	2.83	0.17				3	4.30	5.64							
29	3	2.14	2.81	2	1.99	2.37	1	3.36	4.55	3	3.15	7.15	-1.70	111	456				
				1	1.83	4.56				3	3.57	0.86							
				0.5	2.82	-1.50				3	4.28	4.91							

Table S4. Component Analysis of Pre-edge Features of Cmll Intermediates.

Species	K-edge (eV)	Peak Position (eV)	Peak Area (units)	Ratio
Cmll^R	7122.1	7113.0	0.14	0.1
		7113.1	6.7	4.4
		7114.8	1.5	1.0
	Total = 8.3			
Cmll^{Ox}	7124.1	7113.4	4.9	1.0
		7115.0	9.6	2.0
	Total = 14.5			
Cmll^P	7124.9	7113.7	5.1	1.0
		7114.9	14.1	2.8
	Total = 19.2			

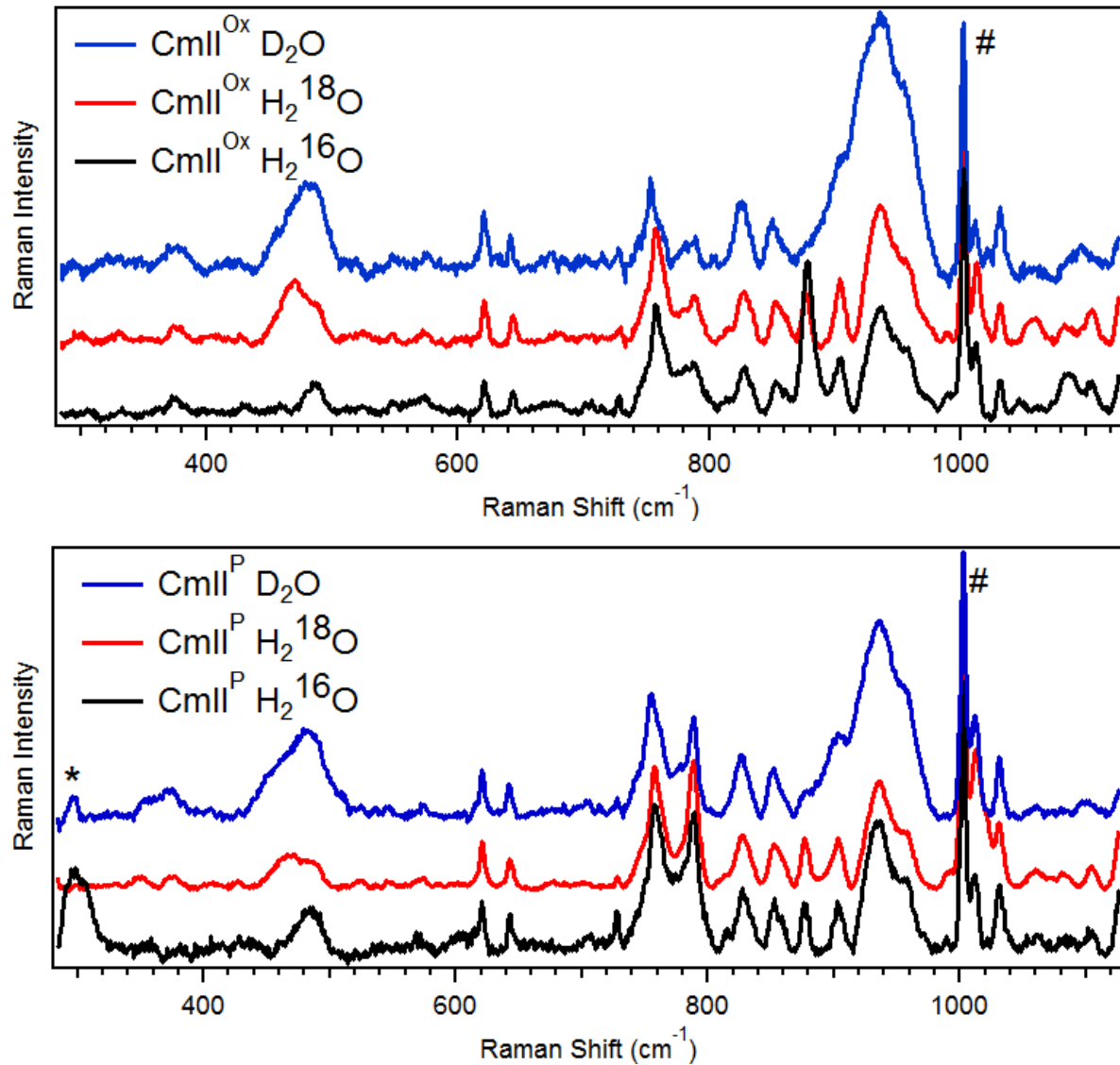


Figure S7. Full resonance Raman spectra for Cmll^{Ox} (top) and Cmll^P (bottom) in H₂¹⁶O (black), H₂¹⁸O (red) and D₂¹⁶O (blue). $\lambda_{\text{ex}} = 561 \text{ nm}$, Power = ~100 mW. All spectra were collected in solution at ~4 °C. Protein concentration ~1 mM for each sample, 50 mM Bicine pH/pD = 9. H₂¹⁸O enrichment of the samples was ~60%. All spectra were normalized to the sharp protein feature at 1002 cm⁻¹ marked with #. Removal of the fluorescence background affected the normalization such that the intensities of the resonance Raman peaks are not necessarily comparable. The peak marked with * is an artifact of the fluorescence background subtraction.